

# Low-temperature resistance and magnetoresistance hysteresis in polycrystalline $(\text{La}_{0.5}\text{Eu}_{0.5})_{0.7}\text{Pb}_{0.3}\text{MnO}_3$

Cite as: J. Appl. Phys. **109**, 053711 (2011); <https://doi.org/10.1063/1.3559303>

Submitted: 22 September 2010 . Accepted: 24 January 2011 . Published Online: 11 March 2011

K. A. Shaykhutdinov, S. I. Popkov, S. V. Semenov, D. A. Balaev, A. A. Dubrovskiy, K. A. Sablina, N. V. Sapronova, and N. V. Volkov



View Online



Export Citation

## ARTICLES YOU MAY BE INTERESTED IN

[Negative magnetoresistance and anomalous Hall effect in GeMnTe-SnMnTe spin-glass-like system](#)

Journal of Applied Physics **113**, 063702 (2013); <https://doi.org/10.1063/1.4790321>

[Fifty years of Anderson localization](#)

Physics Today **62**, 24 (2009); <https://doi.org/10.1063/1.3206091>

[Low-temperature resistivity minimum in ceramic manganites](#)

Journal of Applied Physics **88**, 2578 (2000); <https://doi.org/10.1063/1.1288704>



## Your Qubits. Measured.

Meet the next generation of quantum analyzers

- Readout for up to 64 qubits
- Operation at up to 8.5 GHz, mixer-calibration-free
- Signal optimization with minimal latency

Find out more



## Low-temperature resistance and magnetoresistance hysteresis in polycrystalline $(\text{La}_{0.5}\text{Eu}_{0.5})_{0.7}\text{Pb}_{0.3}\text{MnO}_3$

K. A. Shaykhutdinov,<sup>1,2,a)</sup> S. I. Popkov,<sup>1</sup> S. V. Semenov,<sup>1</sup> D. A. Balaev,<sup>1,2</sup> A. A. Dubrovskiy,<sup>1,2</sup> K. A. Sablina,<sup>1</sup> N. V. Sapronova,<sup>1</sup> and N. V. Volkov<sup>1,2</sup>

<sup>1</sup>Kirensky Institute of Physics, Russian Academy of Sciences, Siberian Branch, Krasnoyarsk, 660036 Russia

<sup>2</sup>Siberian Federal University, Krasnoyarsk, 660041 Russia

(Received 22 September 2010; accepted 24 January 2011; published online 11 March 2011)

The behavior of temperature dependences of electrical resistance and magnetoresistance of polycrystalline substituted lanthanum manganite  $(\text{La}_{0.5}\text{Eu}_{0.5})_{0.7}\text{Pb}_{0.3}\text{MnO}_3$  at low temperatures was thoroughly studied. A broad hysteresis was found in the field dependences of electrical resistance in the low-temperature region. Above 40 K, no hysteresis feature was observed. The temperature  $T = 40$  K corresponds to the temperature of minimum electrical resistance and the temperature  $T_N$  to the antiferromagnet–paramagnet phase transition of the material of the intergrain boundaries. In this work we propose a model which explains the observed features of the  $\rho(T)$  and  $\rho(H)$  curves at temperatures below  $T_N$  by the formation of a network of ferromagnet–antiferromagnet–ferromagnet tunnel contacts. © 2011 American Institute of Physics. [doi:10.1063/1.3559303]

### I. INTRODUCTION

As is known, single-crystal, thin-film, and polycrystalline manganite compounds  $\text{R}_{1-x}\text{A}_x\text{MnO}_3$  where R is a trivalent rare-earth ion, such as  $\text{La}^{3+}$  or  $\text{Pr}^{3+}$ , and A is a divalent ion ( $\text{Ca}^{2+}$ ,  $\text{Sr}^{2+}$ ,  $\text{Ba}^{2+}$ , or  $\text{Pb}^{2+}$ ) exhibit colossal magnetoresistance making these materials promising candidates for practical applications. Upon optimal doping,  $\text{La}_{0.7}\text{Ca}_{0.3}\text{MnO}_3$  single crystals reveal the maximum magnetoresistance near the Curie temperature  $T_c$ , which almost coincides with the temperature  $T_p$  of the metal–dielectric transition. The maximum magnetoresistive (MR) effect is obtained in magnetic fields of several Tesla. In polycrystalline  $\text{R}_{1-x}\text{A}_x\text{MnO}_3$  samples, the maximum magnetoresistance observed below the temperature of the magnetic phase transition depends on various factors, such as grain size, the presence of impurities, and technological conditions.<sup>1,2</sup> The minimum resistance of the polycrystalline manganites is observed at low temperatures;<sup>3–11</sup> the value of the MR effect below the minimum resistance is comparable to, or even exceeds, that observed in the region of the metal–dielectric transition. In addition, in the low-temperature region the presence of a broad hysteresis in the temperature dependences of magnetoresistance and electrical resistance in applied magnetic fields was reported for these materials.<sup>2,3,6,7,10</sup> The origin of the minimum low-temperature resistance and the hysteresis in the  $R(H)$  dependences still has been unclear. In a number of studies,<sup>3–5,7,12</sup> the low-temperature behavior of electrical resistance was explained by spin-dependent tunneling of charge carriers via dielectric spacers separating ferromagnetic grains. The authors of the studies reported in Refs. 8 and 9 analyzed the  $\rho(T,H)$  dependences within a model including the electron–electron interaction and spin-dependent scattering, similar to that observed in the Kondo effect during the interaction between spins of conductivity electrons and localized electrons.

Thus, the low-temperature behavior of electrical resistance and the hysteresis feature observed need detailed experimental study. We propose the following approach to solving the problem. Manganite single crystals are taken as a basis. Their magnetotransport characteristics are thoroughly investigated. Then, the initial single crystals are subjected to grinding, pressing, and annealing to obtain polycrystalline samples in which the crystallites possess properties of the initial single crystals and all the effects typical of the initial single crystals occur at the intergrain boundaries formed during synthesis. As an initial single crystal, we chose a sample with the  $(\text{La}_{0.5}\text{Eu}_{0.5})_{0.7}\text{Pb}_{0.3}\text{MnO}_3$  composition that was synthesized and studied previously.<sup>3,13,14</sup>

In recent work<sup>14</sup> the influence of Eu ions on the A-sites on transport and magnetic properties of the series of  $(\text{La}_{1-y}\text{Eu}_y)_{0.7}\text{Pb}_{0.3}\text{MnO}_3$  crystals ( $y = 0–0.6$ ) have been discussed. The europium ion is of particular interest because it can reveal mixed valence,  $\text{Eu}^{2+}$  and  $\text{Eu}^{3+}$ , in oxides. The trivalent ion in ground state  ${}^7F_0$  ( $J=0$ ), has no magnetic moment (except for the excited state). If some Eu ions in the doped manganite crystals are in divalent state possessing the spin-only moment  $7\mu_B$  ( ${}^8S_{7/2}$ ), these ions can couple with one another or with Mn spins. Thus, physical properties of the manganites doped by Eu ions can essentially differ from those of the crystals doped by other rare-earth ions, revealing, as a rule, 3+ valency in the manganite. However, it turns out<sup>14</sup> that the effective magnetic moment ( $\mu_{\text{eff}}$ ) for all the samples  $(\text{La}_{1-y}\text{Eu}_y)_{0.7}\text{Pb}_{0.3}\text{MnO}_3$  remains approximately constant at doping by Eu ions. Indeed, the ( $\mu_{\text{eff}}$ ) values of the samples obtained from the Curie–Weiss fit are  $\mu_{\text{eff}} = (4.37–4.45)\mu_B$  per formula unit that is very close to spin-only value  $\mu_{\text{eff}} = 4.62\mu_B$  calculated for free  $\text{Mn}^{3+}$  and  $\text{Mn}^{4+}$  ions on the assumption that their ratio corresponds to the formula  $(\text{La}_{1-y}\text{Eu}_y)_{0.7}\text{Pb}_{0.3}[\text{Mn}^{3+}_{0.7}\text{Mn}^{4+}_{0.3}]\text{O}_3$ . This suggests that europium ions in the manganites under investigation are in the trivalent state and do not contribute to the magnetic moment of the samples. Substitution of europium ions with a smaller ionic radius for lanthanum ions induces

<sup>a)</sup>Author to whom correspondence should be addressed. Electronic mail: smp@iph.krasn.ru.

local distortions of Mn-O-Mn bonds in the crystal, which causes random distribution of the value and sign of the exchange interaction over the crystal volume. The competition of exchange interactions leads to the occurrence of inhomogeneous magnetic states in the manganite samples doped by europium ions. The Curie temperature  $T_c$  decreases and the area of the inhomogeneous state existence broadens with increasing Eu concentration. For all the samples, in the area of the inhomogeneous state the colossal magnetoresistance effect is observed. For the crystals with  $x = 0-0.5$  both above and below the temperature of the magnetic phase transition, the paramagnetic phase with polaron conductivity coexists with the ferromagnetic phase with metal conductivity. The sample with  $x = 0.5$  at  $T < T_c$  is in the inhomogeneous state where two ferromagnetic phases with different conductivity coexist. The coexisting phases are observed as spatially separated as a result of frustration of the antiferromagnetic and ferromagnetic interactions at the interface between the phases. The sample with  $x = 0.6$  does not exhibit the maximum resistance at the temperature of the metal-dielectric transition; its resistance grows with decreasing temperature. Correspondingly, the sample with  $x = 0.5$  is at the substitution series edge where the metal-dielectric transition is still observed but the magnetoresistance (MR) effect is maximum. We chose this sample for the measurements of magnetotransport properties.

## II. EXPERIMENTAL

As an initial single crystal, we chose a sample with the  $(\text{La}_{0.5}\text{Eu}_{0.5})_{0.7}\text{Pb}_{0.3}\text{MnO}_3$  composition that was synthesized and studied previously.<sup>3,13,14</sup> In order to prepare polycrystalline  $(\text{La}_{0.5}\text{Eu}_{0.5})_{0.7}\text{Pb}_{0.3}\text{MnO}_3$  samples, the initial single crystals were ground in an agathic mortar, tableted, and annealed for six hours at a temperature of 600°C. The obtained samples possessed sufficient mechanical strength to bear the magnetotransport measurements.

Transport and magnetic measurements were performed on a PPMS-6000 facility and vibrating sample magnetometer at temperatures from 1.9 to 300 K in magnetic fields from 0 to 9 T. Temperature dependences of resistivity  $\rho(H)$  of the polycrystalline  $(\text{La}_{0.5}\text{Eu}_{0.5})_{0.7}\text{Pb}_{0.3}\text{MnO}_3$  samples were taken by a standard four-probe method using samples of  $3 \times 3 \times 0.1$  mm in size.

## III. RESULTS AND DISCUSSION

Scanning electron microscopic (SEM) study of the annealed samples showed an average size of the crystallites of about 1–2  $\mu\text{m}$ . High-resolution transmission electron microscopic study of the grains (Fig. 1) revealed the presence of a 2–3 nm thick surface layer whose structure differs from the structure of the internal volume of the grains. Thus, the surface layer formed during the synthesis serves as an intergrain boundary.

The temperature dependences of resistivity  $\rho(T)$  of polycrystalline  $(\text{La}_{0.5}\text{Eu}_{0.5})_{0.7}\text{Pb}_{0.3}\text{MnO}_3$  for different applied magnetic fields are given in Fig. 2. The inset in the figure presents the temperature dependences of the MR effect  $\Delta\rho/\rho(0)$  for several values of the magnetic field. The  $\rho(T)$

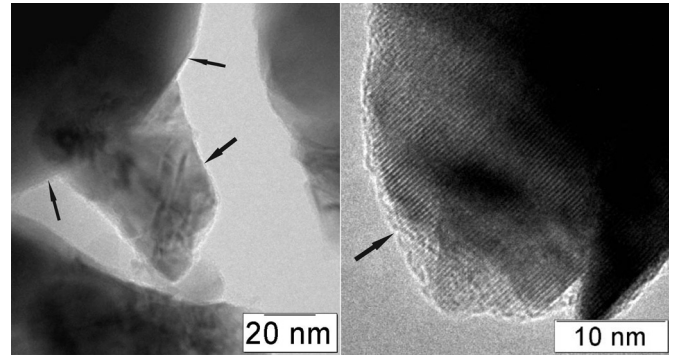


FIG. 1. High-resolution transferring electron microscopy images of polycrystalline  $(\text{La}_{0.5}\text{Eu}_{0.5})_{0.7}\text{Pb}_{0.3}\text{MnO}_3$ . Arrows show the surface layer covering the grains.

dependence of single-crystal  $(\text{La}_{0.5}\text{Eu}_{0.5})_{0.7}\text{Pb}_{0.3}\text{MnO}_3$  was reported in Ref. 3. It is noteworthy the  $\rho(T)$  dependences of the single-crystal and polycrystalline samples are different, as it was mentioned earlier.<sup>15</sup> First of all, there is a shift toward lower temperatures in the metal-dielectric transition for the polycrystalline samples and the difference in absolute values of electrical resistivity related to the presence of the intercrystallite boundaries. In addition, below  $\sim 40$  K the polycrystalline sample exhibits the minimum resistivity; after that, resistivity starts increasing and at helium temperatures reaches values comparable with those for the metal-dielectric transition. The values of the MR effect within the range 2–100 K are practically the same, which is not observed in the case of the single crystals. It should be noted that the shape of  $\rho(T)$  of  $(\text{La}_{0.5}\text{Eu}_{0.5})_{0.7}\text{Pb}_{0.3}\text{MnO}_3$  (Fig. 2) is similar to that of observed for  $\text{La}_{0.77}\text{Ca}_{0.23}\text{MnO}_3$ .<sup>16</sup> Such a form of  $\rho(T)$  (Fig. 2), down to the temperature of low-temperature resistivity minima, can be successfully fit in the frame of the classical model developed in work reported in Refs. 17 and

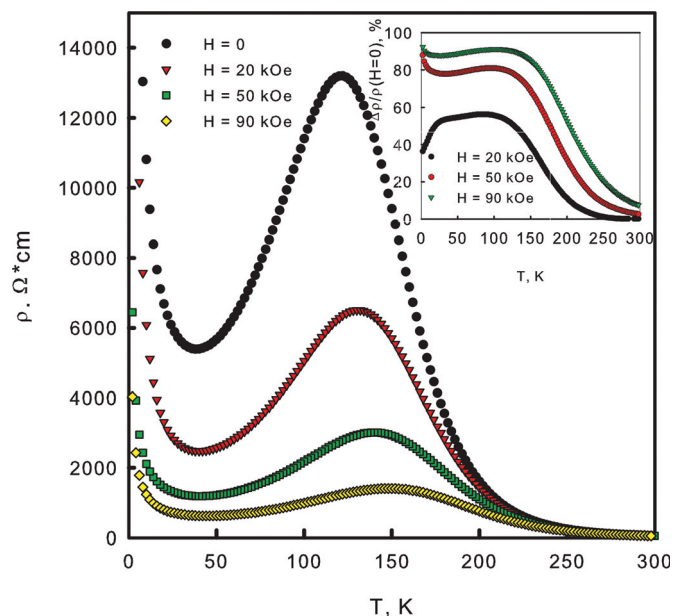


FIG. 2. (Color online) Temperature dependence of resistivity  $\rho(T)$  for polycrystalline  $(\text{La}_{0.5}\text{Eu}_{0.5})_{0.7}\text{Pb}_{0.3}\text{MnO}_3$  sample in different external magnetic fields. Insets show the temperature dependences of the MR effect.

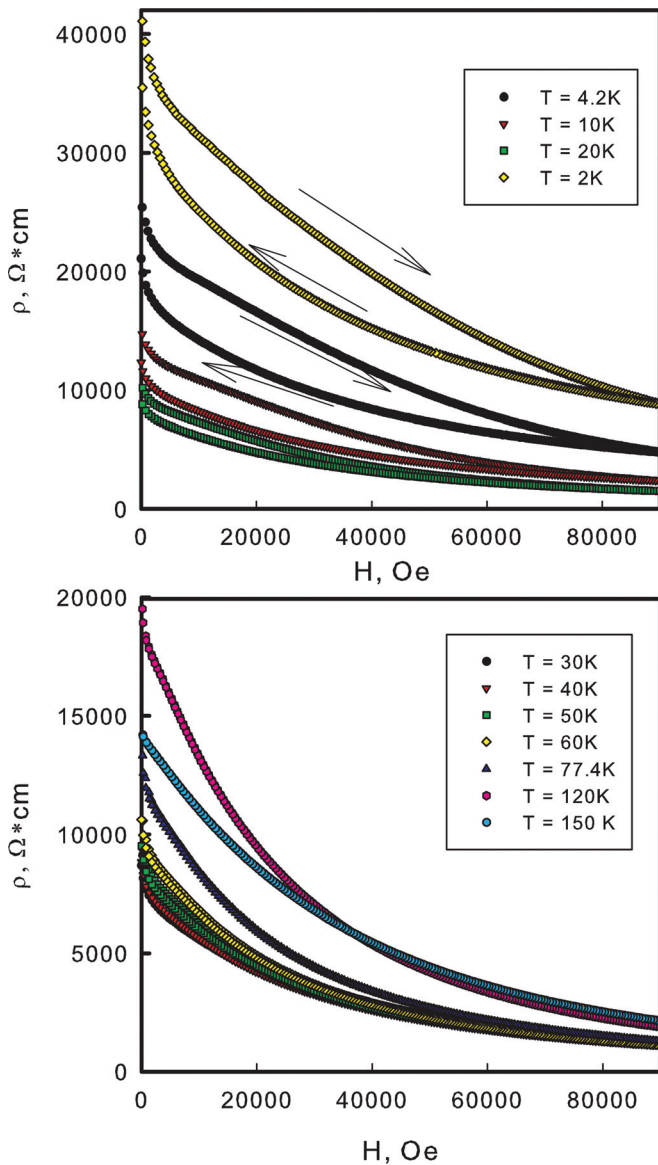


FIG. 3. (Color online) Field dependences for the polycrystalline  $(\text{La}_{0.5}\text{Eu}_{0.5})_{0.7}\text{Pb}_{0.3}\text{MnO}_3$  sample at different temperatures. Arrows point in the direction of motion by the magnetic field  $H$ .

18. However, in the present work we focus attention on the peculiarities of low-temperature magnetoresistance, which is, in our opinion, determined by spin-dependent tunneling of carriers via intergrain boundaries.

Figure 3 demonstrates the  $\rho(H)$  dependences for the polycrystalline  $(\text{La}_{0.5}\text{Eu}_{0.5})_{0.7}\text{Pb}_{0.3}\text{MnO}_3$  sample in a wide temperature range, including the temperature of the metal-dielectric transition and the low-temperature region. The  $\rho(H)$  dependences for the single-crystal  $(\text{La}_{0.5}\text{Eu}_{0.5})_{0.7}\text{Pb}_{0.3}\text{MnO}_3$  sample are not presented here; note, however, that they are typical of the single-crystal lanthanum manganites<sup>15</sup> and have no features in the low-temperature region. The main peculiarities of the  $\rho(H)$  curves (Fig. 3) are the following. First, in the magnetic field  $H \approx 3$  kOe in the range 2–120 K the  $R(H)$  dependence changes; then, resistivity uniformly decreases up to 9 T with no saturation magnetization observed. Second, in the range 2–30 K, i.e., below the temperature of the minimum electrical resistivity, the  $\rho(H)$  curves reveal hysteresis with a

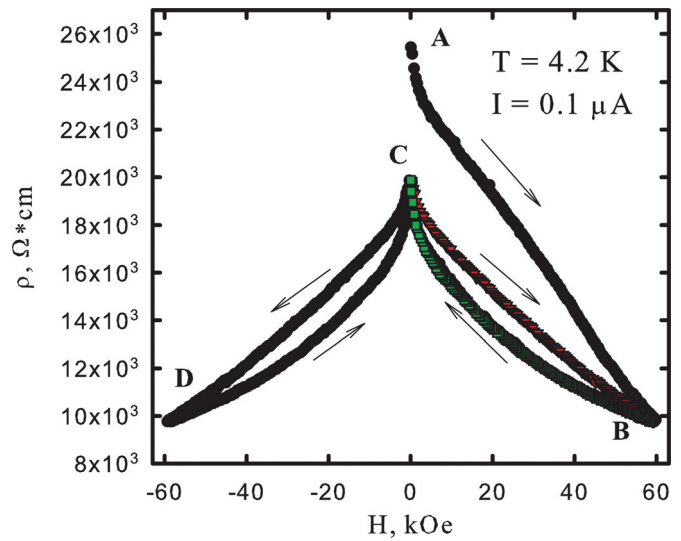


FIG. 4. (Color online) The  $\rho(H)$  dependence for the polycrystalline  $(\text{La}_{0.5}\text{Eu}_{0.5})_{0.7}\text{Pb}_{0.3}\text{MnO}_3$  at  $T = 4.2$  K.

width decreasing with increasing temperature. The direction of the magnetic-field scan is shown by arrows in Fig. 3 (top). Above the temperature of minimum resistivity, no hysteresis features are observed.

Figure 4 depicts the detailed experimental hysteresis dependence of magnetoresistance for the sample under study taken at the temperature  $T = 4.2$  K and the measuring current  $I = 0.1$   $\mu\text{A}$ . In the completely demagnetized state upon zero-field cooling down to room temperature (point A in Fig. 4), the  $\rho$  value is maximum. Portion AB in the figure reflects the magnetoresistance from the completely demagnetized state of the sample to the maximum applied field  $H_{\text{max}} = 60$  kOe. With a decrease in external field down to zero, the  $\rho(H)$  dependence shows a noticeable hysteresis with the  $\rho$  value at  $H \downarrow = 0$  (point C in the figure), much lower than that in the initial demagnetized state. Upon scanning the field to  $H_{\text{max}} = -60$  kOe and back again ( $H \downarrow = 0$ ), which corresponds to portion CD, the hysteresis becomes narrower as compared to that in portion ABC; at point C the resistivity values coincide. With a further increase in field up to  $H_{\text{max}} = +60$  kOe, portion CB of the  $\rho(H)$  dependence is symmetrical to negative branch CD. Upon field cycling to the same value  $H_{\text{max}} = \pm 60$  kOe, the corresponding  $\rho(H \uparrow)$  and  $\rho(H \downarrow)$  dependences are symmetrical relative to the ordinate axis.

The hysteresis dependences of magnetoresistance shown in Fig. 5 were taken under the following conditions: zero-field cooling  $\rightarrow$  field scanning to  $H_{\text{max}} \rightarrow$  decreasing the external field down to  $H \downarrow = 0 \rightarrow$  increasing the external field up to the next  $H_{\text{max}}$  value, again without taking out the magnetic prehistory  $\rightarrow$  decreasing the external field down to  $H \downarrow = 0$ . These measurements were performed at  $H_{\text{max}} = 10, 20, 30, 40, 50,$  and  $60$  kOe and the transport current  $I = 1$   $\mu\text{A}$ . The presented data show that upon field cycling as  $H = 0 \rightarrow H_{\text{max}} \rightarrow H = 0 \rightarrow H_{\text{max}}$  at constant  $H_{\text{max}}$  the  $\rho(H_{\text{max}})$  value is the same; i. e., with an increase in the external field between  $H_{\text{max}} = 10$  kOe and 20 kOe, 20 kOe and 30 kOe, etc. up to  $H_{\text{max}} = 60$  kOe the set of  $\rho(H \uparrow)$  portions coincides with the initial magnetoresistance curve.

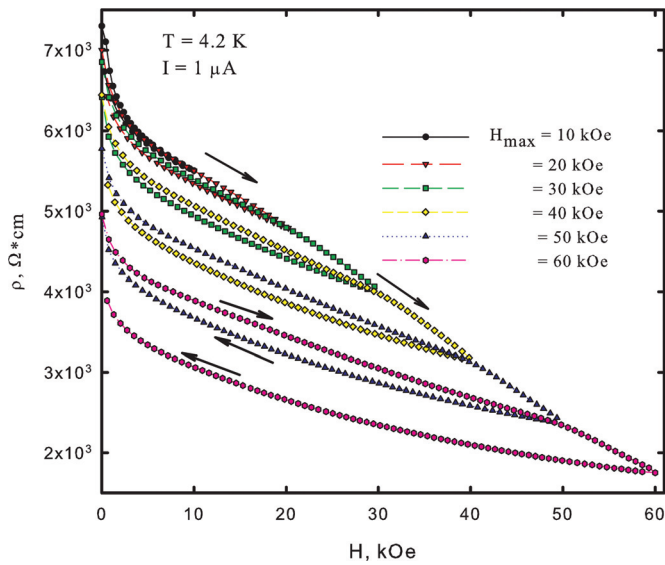


FIG. 5. (Color online) The  $\rho(H)$  dependences for  $(\text{La}_{0.5}\text{Eu}_{0.5})_{0.7}\text{Pb}_{0.3}\text{MnO}_3$  for different values of maximal field  $H_{\text{max}}$ .

The effect of the thermomagnetic prehistory on the  $\rho(T)$  dependence is illustrated in Fig. 6, which depicts the  $\rho(T)$  dependences taken at temperatures up to 60 K upon zero-field cooling and after increasing/decreasing the external field up to 60 kOe at  $T = 4.2$  K. One can see that the thermomagnetic prehistory manifests itself during the resistivity measurements at temperatures up to  $\approx 40$  K.

The behavior of the hysteretic  $\rho(H)$  dependences shown in Figs. 4–6 implies that the sample remembers its magnetic state determined by the maximum applied field. Magnetoresistance is sensitive to the magnetic state. To follow the correlation between the behavior of magnetoresistance and magnetic properties of the sample, magnetization was measured in a way similar to the  $\rho(H)$  measurements.

Figure 7 shows the temperature dependence of magnetization of the  $(\text{La}_{0.5}\text{Eu}_{0.5})_{0.7}\text{Pb}_{0.3}\text{MnO}_3$  sample. As is seen from the  $M(T)$  curve, the Curie temperature  $M(T)$  is nearly

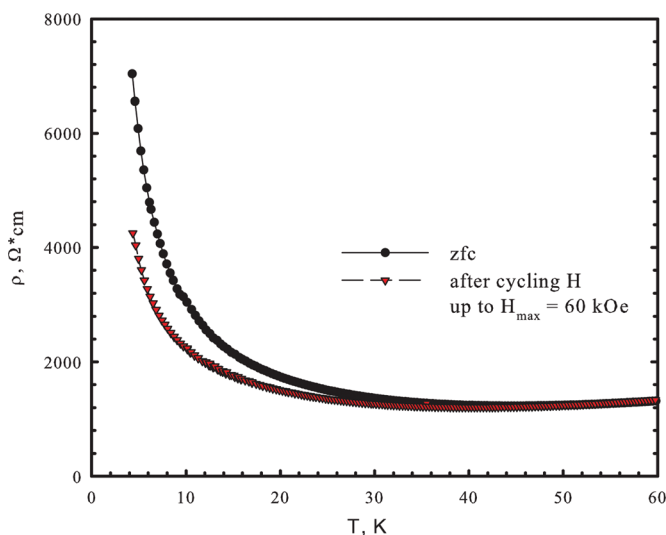


FIG. 6. (Color online) The effect of the thermomagnetic prehistory on the  $\rho(T)$  dependence for the  $(\text{La}_{0.5}\text{Eu}_{0.5})_{0.7}\text{Pb}_{0.3}\text{MnO}_3$ .

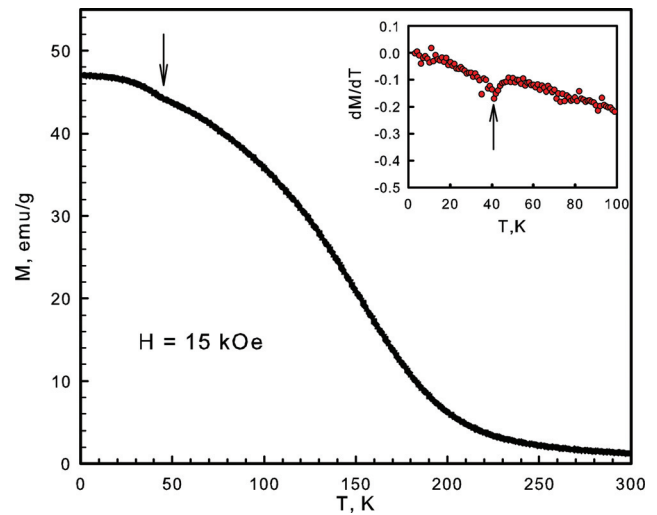


FIG. 7. (Color online)  $M(T)$  dependence for the  $(\text{La}_{0.5}\text{Eu}_{0.5})_{0.7}\text{Pb}_{0.3}\text{MnO}_3$  samples.

215 K. One should note that at  $T = 40$  K the  $M(T)$  curve has a feature corresponding to the magnetic phase transition. This feature is clearly seen in the temperature dependence of the derivative  $dM/dT$  (inset in Fig. 7).

The results of the measurements of low-temperature heat capacity  $C_p(T)$  are shown in Fig. 8. The feature in the  $C_p(T)$  curve at  $T = 40$  K is related to the second-order phase transition occurring in the sample.

The  $M(H)$  dependences taken at temperatures of 4.2 K, 30 K, and 50 K are shown in Fig. 9. At the temperature  $T = 4.2$  K, the  $M(H)$  dependence demonstrates a sufficiently small hysteresis (left inset in Fig. 9; field region near  $H = 0$ ). The  $M(H_{\uparrow})$  and  $M(H_{\downarrow})$  dependences in the strong-field region will be shown below. At the temperature  $T = 30$  K, the  $M(H)$  hysteresis becomes almost indistinguishable within the experimental error; at  $T = 50$  K, the  $M(H)$  hysteresis is absent (right inset in Fig. 9). Such a behavior is consistent with the previously discovered fact<sup>3</sup> that the  $\rho(H)$  hysteresis

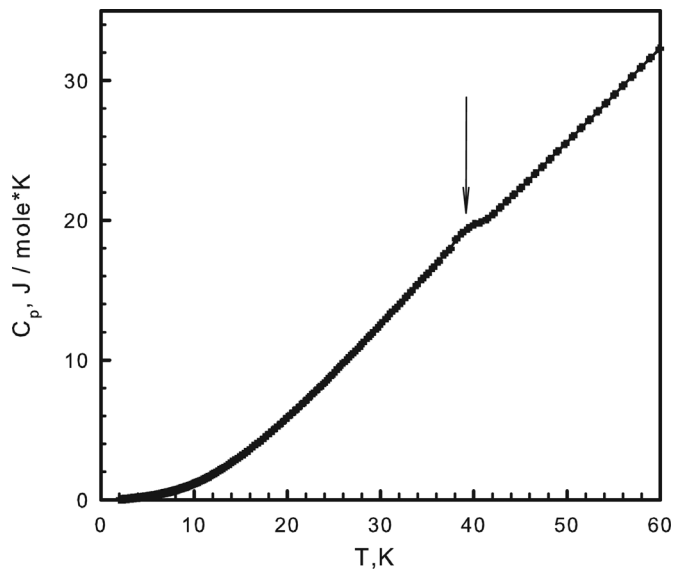


FIG. 8. Temperature dependences of  $C_p$  for the  $(\text{La}_{0.5}\text{Eu}_{0.5})_{0.7}\text{Pb}_{0.3}\text{MnO}_3$ .

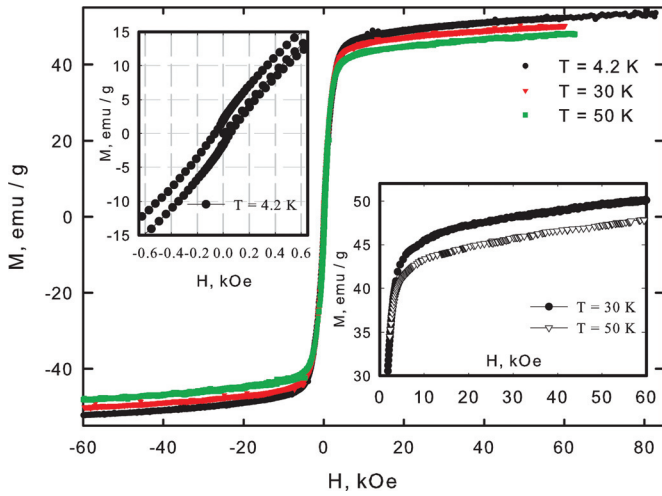


FIG. 9. (Color online) The  $M(H)$  dependences for the  $(\text{La}_{0.5}\text{Eu}_{0.5})_{0.7}\text{Pb}_{0.3}\text{MnO}_3$  at temperatures  $T = 4.2$  K, 30 K, and 50 K.

is maximum at  $T = 2$  K and vanishes at  $T \sim 40$  K. The latter temperature coincides with the Neel temperature of an antiferromagnetic phase (AFM) in the sample that occurs, as was supposed,<sup>19,20</sup> at the grain surface in the sample. Therefore, the temperature regions of existence of the magnetic and magnetoresistive hysteresis nearly coincide. Disappearance of the thermomagnetic prehistory effect at  $T > 40$  K is confirmed also by the  $\rho(T)$  measurements in zero external field (Fig. 6).

Portions of the hysteretic dependences of magnetization taken at  $T = 4.2$  K are shown in Fig. 10. The dependences shown in Figs. 10 and 5 were taken under similar conditions. The prehistory of the  $M(H)$  dependences (Fig. 10) was as follows: zero-field cooling  $\rightarrow$  increasing the field up to  $H_{\text{max}} = 20$  kOe  $\rightarrow$  decreasing the field down to  $H_{\downarrow} = 0$   $\rightarrow$  increasing the field up to  $H_{\text{max}} > 20$  kOe. One can see that upon this variation in the external field the  $M(H)$  dependences

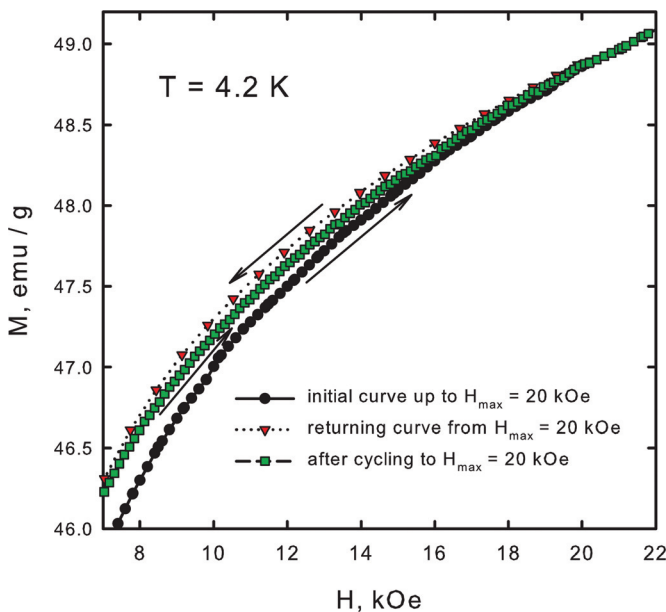


FIG. 10. (Color online) Portions of the hysteretic dependences of magnetization taken at  $T = 4.2$  K.

coincide at the point  $H_{\text{max}} = 20$  kOe; i. e., the  $M(H)$  curve coincides with the initial magnetization curve at the point of the maximum field applied prior to that. The same measurements have been made for  $H_{\text{max}} = 20$  kOe,  $H_{\text{max}} = 30$  kOe,  $H_{\text{max}} = 40$  kOe, and  $H_{\text{max}} = 50$  kOe. Comparing this with the data in Fig. 5, one may conclude that the behavior of the  $M(H_{\uparrow})$  and  $M(H_{\downarrow})$  dependences for different  $H_{\text{max}}$  values is similar to that of the analogous  $\rho(H)$  dependences. The “heights” of the magnetization and magnetoresistance hysteresis  $\Delta M = |M(H_{\uparrow}) - M(H_{\downarrow})|$  and  $\Delta\rho = \rho(H_{\uparrow}) - \rho(H_{\downarrow})$  at  $H_{\uparrow} = H_{\downarrow}$ , grow with  $H_{\text{max}}$ .

It is interesting to compare the  $\Delta M$  and  $\Delta\rho$  dependences. These are shown in Fig. 11 for different  $H_{\text{max}}$ . In Fig. 11, the thermomagnetic prehistory for the magnetic and magnetoresistive data is the same. A comparison of Figs. 11(a) and 11(b) reveals the correlation between dependences: steep  $\Delta M$  and  $\Delta\rho$  growth is observed in the small-field region. However, comparing  $\Delta M$  and  $\Delta\rho$  behavior at a certain value of the external field, one can see that the  $H_{\text{max}}$  value affects the  $\Delta M(H_{\text{max}})$  and  $\Delta\rho(H_{\text{max}})$  dependences differently. The insets in Figs. 11(a) and 11(b) show the  $\Delta M(H_{\text{max}})$  and  $\Delta\rho(H_{\text{max}})$  dependences at the fixed fields  $H = 0$  and  $H = 5$  kOe. The “height” of the  $M(H)$  hysteresis changes slightly with increasing  $H_{\text{max}}$ , at least, starting from  $H_{\text{max}} = 10$  kOe, and the  $\Delta M(H_{\text{max}})$  dependence has negative curvature, whereas the “height” of the  $\rho(H)$  hysteresis grows with  $H_{\text{max}}$  fairly fast and the  $\Delta\rho(H_{\text{max}})$  dependence has positive curvature.

Thus, despite the fact that hysteretic dependences of magnetization and magnetoresistance are qualitatively identical, parameters  $\Delta M$  and  $\Delta R$  characterizing the hysteresis

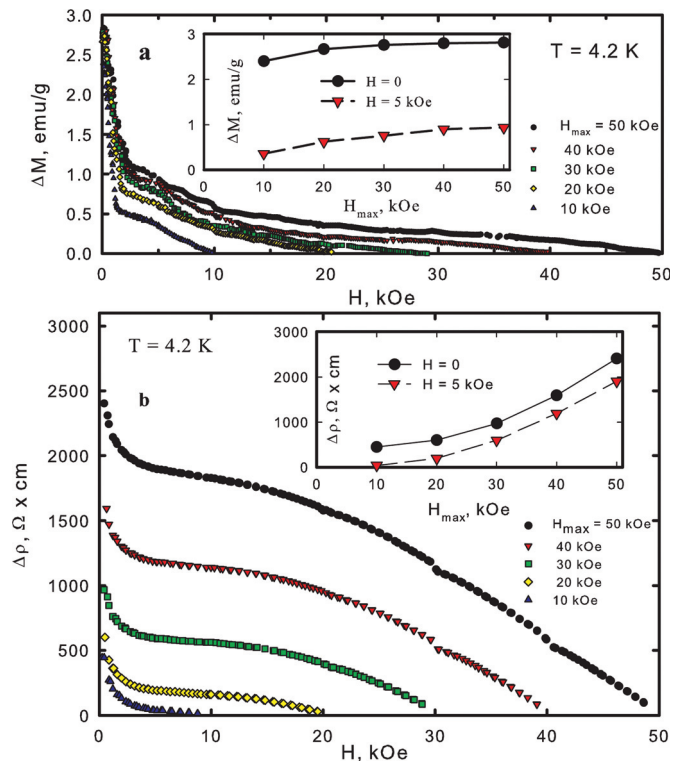


FIG. 11. (Color online) The “heights” of the magnetization and magnetoresistance hysteresis (a)  $\Delta M = |M(H_{\uparrow}) - M(H_{\downarrow})|$  and (b)  $\Delta\rho = \rho(H_{\uparrow}) - \rho(H_{\downarrow})$  at  $H_{\uparrow} = H_{\downarrow}$ .

are nonlinearly dependent. In addition, as was mentioned above, the  $M(H)$  hysteresis is rather narrow, while the  $R(H)$  dependence exhibits pronounced hysteresis.

Now, let us analyze the results obtained. It was reported previously<sup>3</sup> that the  $M(H)$  hysteresis of initial single crystals of this composition is considerably lower than that of the polycrystalline sample under study. The antiferromagnetic phase with  $T_N \sim 40$  K forming at the grain surface<sup>3</sup> cannot contribute to the hysteresis. This means that a small amount of one more “magnetic phase” arises in the polycrystalline sample, which causes a relatively small yet observable  $M(H)$  hysteresis and is responsible for the hysteretic behavior of magnetoresistance.

We propose the following model for description of the  $R(H)$  and  $M(H)$  hysteresis. A grain core remains ferromagnetic (measuring temperature is much lower than  $T_c$ ), while at the grain surface the AFM phase forms. Since the grain size, according to the SEM data, is  $\sim 10^2$ – $10^3$  nm, a linear size of the AFM spacer is estimated as  $\sim 2$ – $3$  nm. The remainder of the grain core volume is sufficient for the formation of a domain structure. Therefore, the FM phase has the domain structure; the domains neighboring the AFM phase, hereinafter referred to as N-domains, may be exchange-coupled with both this phase and FM domains composing the grain core. For the domains neighboring the AFM covering, the exchange interactions with AFM and FM phases may compete. The exchange with the ferromagnetic phase favors rotation of the magnetic moment with the field, while the exchange with the AFM phase may prevent ordering. As a result, the energy of the magnetic moments of the N-domains may have local minima points as in spin or spin-cluster glass. Obviously, an increase in the external field facilitates hopping over potential barriers and, upon cycling, the hysteresis is observed. Narrowness of the  $M(H)$  hysteresis says that it is formed by a small fraction of the ferromagnetic phase. According to the  $M(H)$  data (Fig. 9), the fraction of the N-domains is only  $\sim 5\%$ , which yields a linear size of the N-domains of about 10 nm at a grain diameter of 1  $\mu\text{m}$ .

The proposed model may explain the  $R(H)$  hysteresis if magnetoresistance is considered to be caused by tunneling carriers via dielectric spacers. Tunneling of electrons via the AFM spacer and magnetoresistance is determined not by orientation of the magnetic moments of grain cores but by mutual orientation of the magnetic moments of the N-domains. The change in  $R(H)$ , similar to the change in  $M(H)$ , is maximum from the completely demagnetized state with the maximum resistivity in weak fields (up to  $\sim 5$  kOe), but in the field region 20–60 kOe magnetoresistance is also considerable, whereas the  $M(H)$  dependence grows slightly in this region. The contribution of the N-domains to the resulting magnetization of the sample is relatively small (total magnetization is apparently determined by superposition of the contributions of the FM and AFM phases and the N-domains). Therefore, the processes of alignment of the N-domains along the field determine the behavior of the

$R(H)$  dependence. The narrow  $M(H)$  hysteresis is revealed in the considerable magnetoresistance hysteresis. Above we demonstrated the correlation between the  $R(H)$  and  $M(H)$  hysteretic parameters and the behavior of the  $R(H)$  and  $M(H)$  dependences at the magnetic prehistory. The positive and negative branches of the magnetoresistance hysteresis (CB and CD in Fig. 4) are symmetrical because in the magnetic tunneling processes the states with positive and negative residual magnetization are identical.

## IV. CONCLUSION

Thus, this proposed model explains qualitatively the low-temperature behavior of the temperature dependences of electrical resistivity and magnetoresistance of polycrystalline  $(\text{La}_{0.5}\text{Eu}_{0.5})_{0.7}\text{Pb}_{0.3}\text{MnO}_3$  by the formation of a network of ferromagnet-antiferromagnet-ferromagnet tunnel contacts in the low-temperature region.

This study was partially supported by the Russian Foundation for Basic Research, Project No. 08-02-00259a and the Lavrentyev Competition of the Young Scientists’ Projects of the Siberian Branch of the Russian Academy of Sciences, Project No. 12.

<sup>1</sup>P. Dey and T. K. Nath, *Phys. Rev. B* **73**, 214425 (2006).

<sup>2</sup>M. Pekala, N. Kozlova, and V. Drozd, *J. Appl. Phys.* **104**, 123902 (2008).

<sup>3</sup>K. A. Shaykhutdinov, S. I. Popkov, S. V. Semenov, D. A. Balaev, A. A. Dubrovskiy, K. A. Sablina, and N. V. Volkov, *J. Phys.: Conf. Ser.* **200**, 052025 (2010).

<sup>4</sup>E. Rozenberg, M. Auslender, I. Felner, and G. Gorodetsky, *J. Appl. Phys.* **88**, 2578 (2000).

<sup>5</sup>M. Auslender, A. E. Kar’kin, E. Rozenberg, and G. Gorodetsky, *J. Appl. Phys.* **89**, 6639 (2001).

<sup>6</sup>J. H. Miao, S. L. Yuan, X. Xiao, G. M. Ren, G. Q. Yu, Y. Q. Wang, and S. Y. Yin, *J. Appl. Phys.* **101**, 043904 (2007).

<sup>7</sup>K. A. Shaykhutdinov, S. V. Semenov, D. A. Balaev, M. I. Petrov, and N. V. Volkov, *Phys Solid State* **51**, 778 (2009).

<sup>8</sup>Y. Xu, J. Zhang, G. Cao, C. Jing, and S. Cao, *Phys. Rev. B* **73**, 224410 (2006).

<sup>9</sup>D. Kumar, J. Sankar, J. Narayan, R. K. Singh, and A. K. Majumdar, *Phys. Rev. B* **65**, 094407 (2002).

<sup>10</sup>P. K. Muduli, G. Singh, R. Sharma, and R. C. Budhani, *J. Appl. Phys.* **105**, 113910 (2009).

<sup>11</sup>A. Gupta, G. Q. Gong, G. Xiao, P. R. Duncombe, P. Lecoeur, and P. Trouilloud, *Phys. Rev. B* **54**, R15629 (1996).

<sup>12</sup>P. Chowdhuru, S. K. Gupta, N. Padma, C. S. Viswanadham, S. Kumar, A. Singh, and J. V. Yakhmi, *Phys. Rev. B* **74**, 014434 (2006).

<sup>13</sup>N. Volkov, G. Petrakovskii, K. Patrin, K. Sablina, E. Eremin, V. Vasiliev, A. Vasiliev, M. Molokeev, P. Boni, and E. Clementyev, *Phys. Rev. B* **73**, 104401 (2006).

<sup>14</sup>N. Volkov, G. Petrakovskii, P. Boni, E. Clementyev, K. Patrin, K. Sablina, D. Velikanov, and A. Vasiliev, *J. Magn. Magn. Mater.*, **309**, 1 (2007).

<sup>15</sup>*Colossal Magnetoresistive Oxides*, edited by Y. Tokura, (Gordon and Breach Science Publishers, New York, N.Y., 2000).

<sup>16</sup>Y.-Q. Li, J. Zhang, S. Pombrik, S. DiMascio, W. Stevens, Y.F. Yan, and N. P. Ong, *J. Mater. Res.* **10**, 2166 (1995).

<sup>17</sup>G. F. Dionne, *J. Appl. Phys.* **79**, 5172 (1996).

<sup>18</sup>G. F. Dionne, *Magnetic Oxides* (Springer, New York, N.Y., 2009).

<sup>19</sup>M. J. Calderon, L. Brey, and F. Guinea, *Phys. Rev. B* **60**, 6698 (1999).

<sup>20</sup>J. Salafranca, M. J. Calderon, and L. Brey, *Phys. Rev. B* **77**, 014441 (2008).